SIGNAL DETECTION AND ESTIMATION AT THE NEW INTERNATIONAL MONITORING SYSTEM ARRAY AT MINA

Jin Wang, Hans Israelsson, Keith McLaughlin
Center for Monitoring Research, SAIC

Sponsored by U.S. Department of Defense
Defense Threat Reduction Agency
Contract No. DTRA01-99-C-0025

ABSTRACT

The Mina seismic array, NVAR, in Nevada was recently put into operation and added to the so International Monitoring System (IMS). NVAR includes two seismic subarrays, one with 10 and one with 3 elements. With a diameter of about 5 km and equipped with short period vertical instruments, the 10 element subarray is designed primarily for detection of regional phases and teleseismic P phases. The 3 element subarray lends itself to processing of surface waves with its three-component broad band instruments. It has a diameter of about 20 km and is symmetrically centered around the smaller 10 element array. An additional three component element (NV11) provides, by virtue of its co-location with the conventional station MNV, continuity with historic data.

In this paper we assess the performance of NVAR during its initial few months of operation as part of the IMS using data forwarded to and processed real-time at the Prototype International Data Center (PIDC). Beamforming, signal detection, frequency-wavenumber (f-k) analysis and other types of processing were initially set up according to standard procedures developed at the PIDC.

During the period Feb. 19 - May 18, 1999, an average of 60 signals/day were detected by the automatic processing for NVAR. About one quarter of the detections were subsequently associated with seismic events of the Reviewed Event Bulletin, REB, published by the PIDC, whereas about only 3 signal/day, were missed by the automatic system, had to be added during analyst review for NVAR. This performance is quite comparable to that of similar arrays, like the Pinedale array in Wyoming and the TXAR array in Texas, which have been operating for some time and have benefited from tuning of their processing. Furthermore, the number of signals associated with events in the REB for NVAR almost doubled compared with that of the conventional station MNV.

The slowness and azimuth estimation of detected signals, based on f-k analysis, shows large systematic bias, of up to 3 sec/degree, throughout the slowness plane for NVAR. This can be attributed to the relatively large range in elevation (about 500 m) spanned by array elements and the assumption of co-planar location of array elements in the f-k algorithm. The PIDC processing scheme does, however, allow for removal of slowness bias by applying corrections to observed slowness. Development of such corrections for NVAR is currently in progress, which together with evaluation of other aspects of the NVAR real-time processing will likely lead to fine-tuning of several processing configurations. This will, in turn, most probably enhance the performance of NVAR, which already in its initial few months of operation shown encouraging results with the default configuration.

Key Words: CTBT, Array Detection, Signal Processing

INTRODUCTION

The Nevada Array (NVAR) is the last and newest IMS primary station to be added to North America and the closest primary IMS station to the historically important US Nevada Test Site (NTS). The IMS network is almost complete for North America. NVAR began contributing to the PIDC Reviewed Event Bulletin (REB) on February 17, 1999. The site includes the three-component (3C) Mina Nevada (MNV) station which ceased contributing to the REB on April 14, 1999. This paper reports on preliminary evaluation of the first few months of NVAR operation. The upgrade from MNV to NVAR was anticipated to improve detection and location in North America. IDC automatic processing depends heavily upon arrays to form initial events. The automatic detection, phase identification, and association of array signals is critical to this processing. Arrays generally have lower detection thresholds, higher SNR, better phase identification, and contribute more reliable back-azimuths for association, and location.

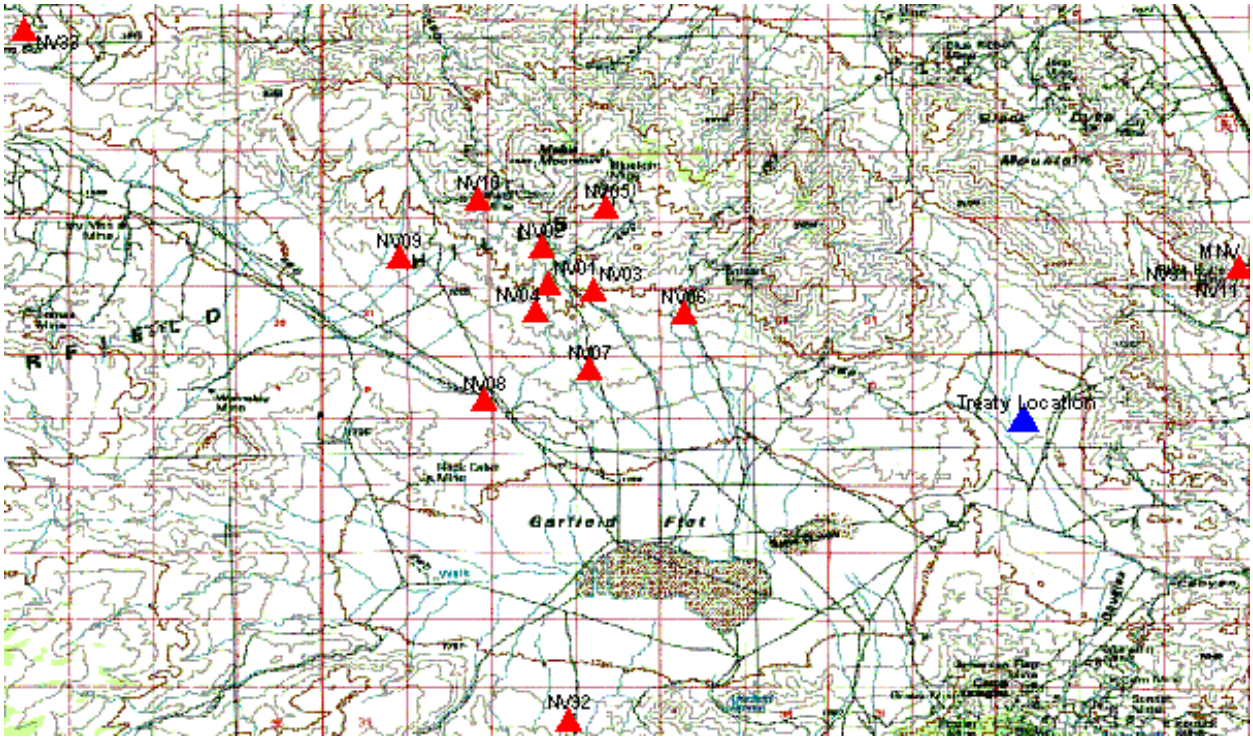

Figure 1. Map of the Nevada Array (NVAR) showing the inner 10 element short period array and the outer 3 element broadband array. The inner 10 element array is built upon the side of a mountain with elevation differences of almost 500 meters.

ARRAY CONFIGURATION

Figure 1 is a topographic map of the array NVAR. From the map we can see that NVAR includes two seismic subarrays, one with 10 and one with 3 elements. With a diameter of about 5 km and equipped with short period vertical instruments, the 10 element subarray is designed primarily for detection of regional and teleseismic P phases. The 3 element subarray lends itself to processing of surface waves with its three-component broad band instruments. It has a diameter of about 20 km and is symmetrically centered around the smaller 10 element array. An additional three component element (NV11) provides, by virtue of its co-location with the conventional 3 component station MNV, continuity with historic data.

Figure 2 shows the instrument displacement response curves for the short-period and broadband instruments installed in NVAR. The curves are normalized at 1 Hz frequency. The broadband KS54000M101 is flat to acceleration up about 5 Hz. The short period GS-13 instrument is flat to velocity above 1 Hz.

The beamforming detectors of NVAR were configured using a systematic approach previously developed at the PIDC (Wang et al., 1996). This approach takes into account array geometry, slowness and frequency distribution of seismic signals, and coherency properties between sensor sites. Figure 3 shows the positions of steered-beams in the slowness plane for signal detection.

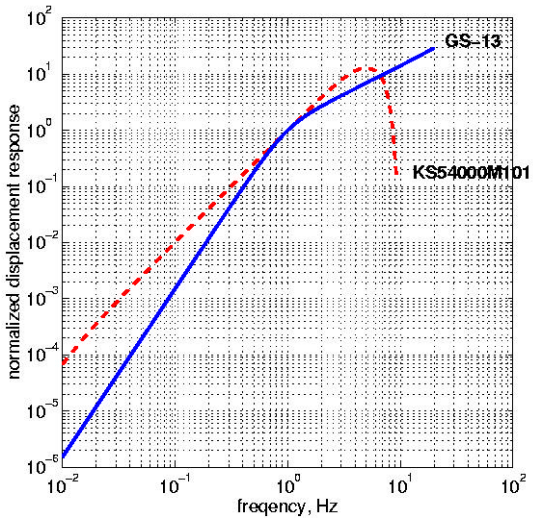

Figure 2: Instrument response at NVAR. The solid line shows the displacement response of the short-period seismometer GS-13. The dashed-line shows the displacement response of the broadband seismometer KS54000M101. The GS-13 anti-alias filter is not included.

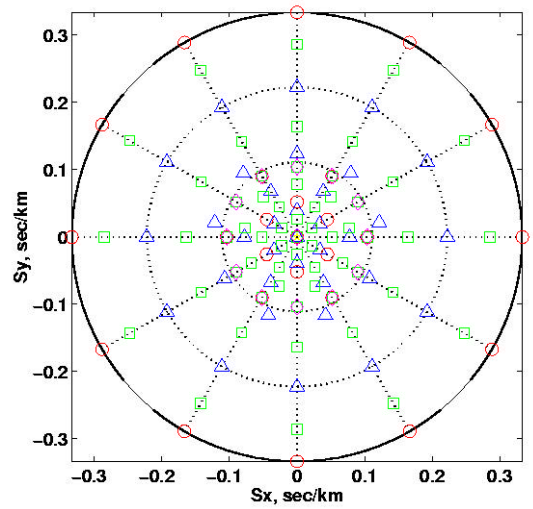

Figure 3: Detection beam deployment at NVAR in the slowness-azimuth plane. Different symbols represent the slowness positions in different frequency bands (circles: 0.75-2.25 Hz; triangles: 1.0 to 3.0 Hz; squares: 2.0-4.0 Hz; diamonds: 3.0-6.0 Hz; pentagrams: 4.0-8.0 Hz).

SIGNAL DETECTION AND ASSOCIATION

The IDC software performs STA/LTA detection on each individual beam. Each beam has a threshold to declare detections. Based on previous experience with other stations, the current initial thresholds at NVAR range from 3.5 to 5.5. These thresholds are tunable after a period of operation. Table 1 shows metrics for detection performance of NVAR for a period of three months (from February 19, 1999 to May 18, 1999). For comparison, the performances for the three-component station MNV, which is co-located with the sensor NV11, of three months (from December 19, 1998 to March 18, 1999) and for three similar arrays, GERES, PDAR, and TXAR are also listed in Table 1. In the table, "# of detection/day" represents the average number of detections per day by the automatic system (Standard Event List 3, SEL3). It should be mentioned that most of the automated detections were identified as 'noise' detections by the automated system. Those 'noise' detections would not be further processed by the automated system. The second row shows the average number of 'signal' detections (total detections excluding 'noise' detections) per day. The third row represents the average number of detection associated in the final Reviewed Event Bulletin (REB). The fourth row represents the number of phases, that were missed by the automatic system, and added during analyst review. The fifth row represents the number of detections, that were incorrectly associated by the automatic system, and removed by analysts. From the table we see that NVAR outperforms the 3C station MNV on each statistic, and has comparable detection performance to that of other similar arrays.

Table 1. Detection performance of NVAR and comparison with other stations

Metric	MNV	NVAR	GERES	PDAR	TXAR
# of detection/day	342.2	281.4	368.9	269.1	285.4
# of signal/day	218.6	64.7	235.1	194.9	135.5
# of associated in REB/ day	6.5	16.9	17.3	17.5	15.7
# of added/day	0.9	3.2	2.1	3.1	4.2
# of dis-associated/day	11.4	9.0	22.4	26.8	18.5

Table 2 compares initial phase identification and event association for NVAR, MNV, GERES, PDAR, and TXAR. The first row represents the performance of initial phase identification. The automatic system at the PIDC uses rules for arrays and default neural networks for 3-C stations to classify initial phase types. From the table we can see that NVAR outperforms the 3-C station MNV for initial phase identifications but performs less well than the other three arrays. We believe this is because of bias in slowness estimation at NVAR, which is discussed in the next section. For event formation and detection, NVAR detected 83.5% and 40.0% of regional events and teleseismic events, respectively, while MNV detected only 62% and 19% of regional events and teleseismic events, respectively. Detection at three or more primary station are required for an event to appear in the REB. The last row of Table 2, 'contribution to 3- station-events', compares the contribution to such three-station events for NVAR and the other stations. Without detections at NVAR, 9 of the 387 events during the three month period would not have appeared in the REB, whereas no event was critically dependent on detection at MNV.

Table 2. Association performance of NVAR and comparison with other stations

Metric	MNV	NVAR	GERES	PDAR	TXAR
% of unchanged initial phase type	72.7	78.3	92.9	97.2	97.2
% of regional events detected	62.0	81.0	68.0	72.0	76.0
% of teleseismic events detected	19.0	44.0	37.0	50.0	55.0
contribution to 3-stations events (associated/total)	0/433	9/387	10/387	14/387	25/387

SLOWNESS AND AZIMUTH ESTIMATION

Seismic arrays usually have better slowness and azimuth estimation than 3-C stations. However, NVAR has a larger systematic bias than MNV, with a median slowness residual of 3.0 sec/degree as shown in Table 3.. It also has larger slowness bias than the other similar arrays. Figure 4 shows the slowness-azimuth error vector map in the slowness-azimuth plane for all NVAR associated phases. To limit the effect of small signal-to-noise ratio (SNR) on the analysis, Figure 5 shows slowness-azimuth error vectors for NVAR associated phases with SNR>=8. From this figure we can see that there are two major trends for the error vectors. One is southeast and another is southwest. These biases are clearly not caused by low SNR. The IDC software can remove slowness bias by applying Slowness-Azimuth Station Corrections (SASC). They are usually derived from observed slowness and azimuth residuals (Bondár, 1998). As a new station, NVAR has no SASC available at this time. Table 3 demonstrates the SASCs have reduced estimation biases at MNV and other three similar arrays.

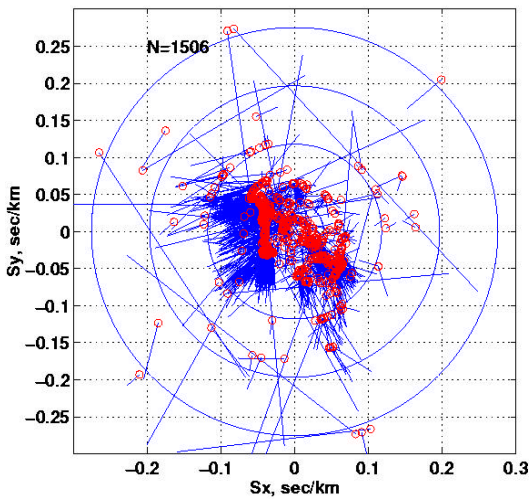

Figure 4. Slowness-Azimuth error vector map in the slowness-azimuth plane for all NVAR associated phases in REB. Circles represent predicted values and tails represent observed values.

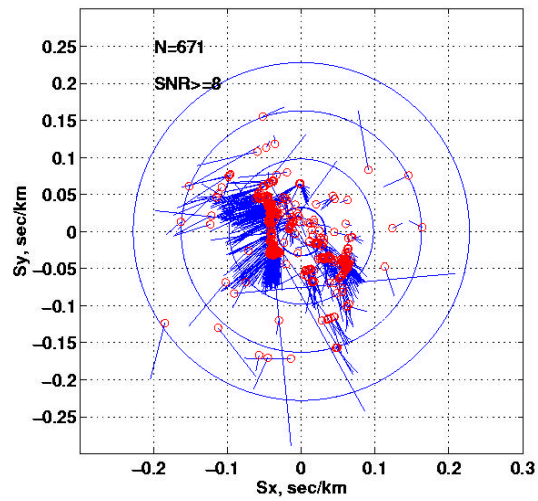

Figure 5. Slowness-Azimuth error vector map in the slowness-azimuth plane for NVAR associated phases in REB with SNR>=8. These vectors show two trends of biases. One in southeast and the other is southwest.

Table 3. Slowness-Azimuth estimation of NVAR and comparison with other stations

	MNV	NVAR	GERES	PDAR	TXAR
Median of slores, sec/deg	-1.29	3.00	-0.24	-1.10	-0.29
Std of slores, sec/deg	2.83	2.48	1.26	2.05	2.11
Median of slores with SASC, sec/deg	-0.51	N/A	-0.11	-0.54	-0.18
Std of slores with SASC, sec/deg	3.04	N/A	1.23	1.47	1.08
Median of azires, deg	3.3	-2.8	2.3	-9.0	-12.8
Std of azires, deg	35.0	21.8	14.5	28.1	26.6
Median of azires with SASC, deg	3.3	N/A	1.7	-0.6	-0.6
Std of azires with SASC, deg	34.4	N/A	14.5	15.5	9.6

ELEVATION EFFECTS AND CORRECTIONS

The current beamforming and f-k analysis algorithms at the PIDC assume that all elements of an array are located in the same horizontal plane so that time delays among all sensors are determined by their horizontal locations. There are no elevation corrections made to the beams. For most IMS arrays, the algorithm works fine because of small elevation differences. However, the relatively large range in elevation at NVAR (about 500 meter difference over 5000 meters aperture) has significant effects on signal propagation and processing.

Assuming all elements are in the same plane, the time delay of the signal at the *i*-th sensor with respect to a reference sensor will be:

$$\tau'_i = (x_i * s_x + y_i * s_y), \qquad (1)$$

where (x_i, y_i) are the 2-D spatial coordinates of the i-th sensor with respect to the reference sensor, and (s_x, s_y) are slowness components in x, y directions, respectively. However, the actual time delay because of elevation differences is:

$$\tau_i = x_i * s_x + y_i * s_y + z_i * s_z , \qquad (2)$$

where z_i is the elevation difference with respect to a reference sensor, and s_z is the vertical slowness component which is constrained by phase velocity, V, of the propagating signal:

$$V^{-1} = \mathrm{sqrt}(s_x^2 + s_y^2 + s_z^2) \qquad (3)$$

Figure 6 shows the array response, or so-called beam-pattern, of NVAR for a vertically incoming signal ($s_x = 0$ and $s_y = 0$) at frequency 1 Hz, taking into account elevation differences and assuming V = 4.0 km/sec. The contours are normalized with respect to the maximum at 0.1 intervals. If the array is in a perfect horizontal plane, the peak of the response will be located at the center. From figure 6 we can see that the peak of the elevation effect beam pattern is shifted to the south direction. It also can be noticed from Figure 6 there are two local maxima. One local maximum is greater than 0.7 of amplitude of the main peak. The system may pick the second maximum as the slowness position of incoming signals, which is shifted to the southwest. It should be mentioned that the beam-pattern shown in Figure 6 was computed for all 11 'sz' sensors in NVAR. Figure 1 shows NV11 is far from the other 10 'sz' sensors and it should not be included in the signal processing (beamforming and f-k analysis) because of lacking signal coherence with the other 10 'sz' sensors. Beamforming can be computed with any sensor group and the current initial beamforming group consists of the 10 closely spaced sensors. For F-k analysis, however, the automatic system only can group sensors by their instrument type, that is to say, all 11 'sz' channels in NVAR are used for f-k analysis. This beam-pattern explains the two bias trends in figures 4 and 5. Figure 7 shows the elevation effected beam-pattern of NVAR with only 10 closely spaced sensors. It shows that the local maxima have disappeared but it is still biased by 0.035 sec/km (or 3.9 sec/deg) to the south.

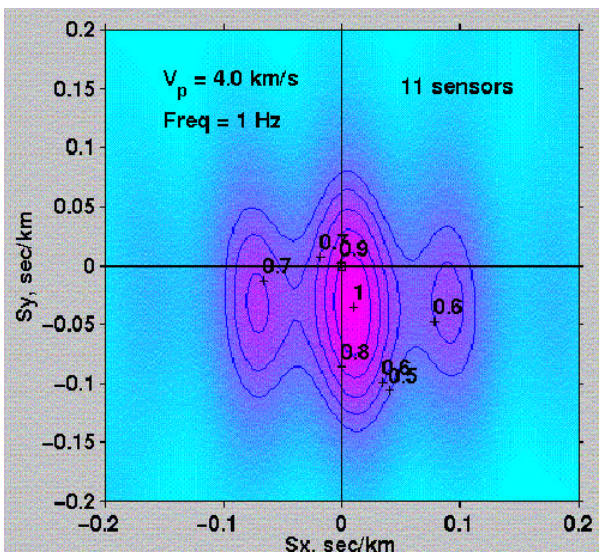

Figure 6. Beam pattern of NVAR with all 11 short-period sensors. It shows the main peak is shifted toward south direction because of elevation differences. It also shows there is one local maximum which is greater than 0.7 in the southwest direction.

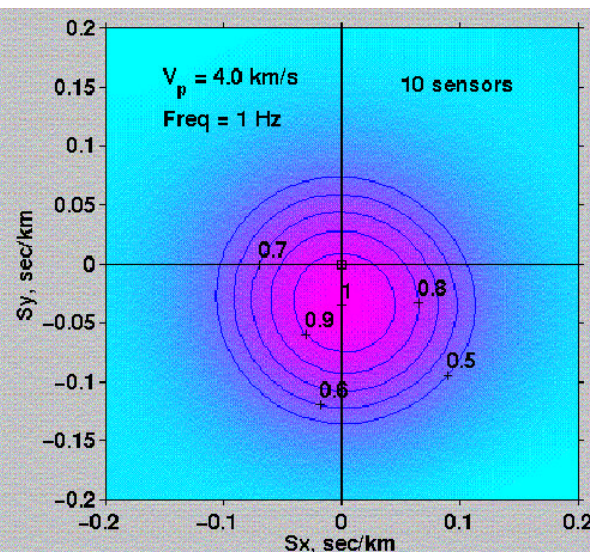

Figure 7. Beam pattern of NVAR with 10 short-period sensors which are closely located. It shows the main peak is shifted toward the south direction and the contours become simple concentric circles.

We can estimate slowness and azimuth residues introduced by ignoring the elevation differences at NVAR. In the current f-k algorithm, the peak in the f-k spectrum indicates the best matched time delays which are used to derive the slowness and azimuth of a signal across the array. By assuming signal phase velocity Vp, the relation between the true slowness vector and observed vector is given by:

$$\begin{matrix} x_1 & y_1 & z_1 \\ x_{i=2,3} & y_{i=2,3,\ldots} & z_{i=2,3,\ldots} \\ x_N & y_N & z_N \end{matrix} \begin{matrix} s_x \\ s_y \\ s_z \end{matrix} = \begin{matrix} x_1 & y_1 \\ x_{i=2,3} & y_{i=2,3,\ldots} \\ x_N & y_N \end{matrix} \begin{matrix} s_x' \\ s_y' \end{matrix} \quad (4)$$

where N is the number of sensors, (s_x, s_y) are true slowness and (s_x', s_y') are observed slowness when ignoring elevation effect. Figure 8 shows the predicated slowness-azimuth residue vectors induced by elevation effects at NVAR. The circles represent the true incoming slowness-azimuth, the tails represent observed slowness-azimuth. The residues vary with incoming slowness and azimuth values in a systematic way.

Not only do the elevation differences yield distorted array response, but they also cause reduced array gain because of mismatched delays. The differences between τ_i and τ'_i are called mismatched delays. Mismatched delays reduce the signal-to-noise ratio at the beamforming output, thereby reducing the array gain. The array gain in the case of mismatched delays can be estimated if we assume the signal is a monochromatic plane wave (Johnson and Dudgeon, 1993). Figure 9 shows the array gains normalized by the gain at a perfect matched delay for a 10-sensor subarray of NVAR. It shows the theoretical array gain drops quickly for high frequency bands, and also drops with decreasing slowness. For 0.01 sec/km slowness, the effectiveness of the array at 2 Hz is reduced to 70% and 30% at 4 Hz by the elevation effects alone.

Given the large predicted effects of elevation on array gain we have experimented with elevation corrections for beamforming at NVAR on observed signals. In these experiments, time delays are determined by equation (2) assuming the predicated slowness and azimuth in REB are the true values and the phase velocity of signals underneath the NVAR is 4.0 km/sec. The preliminary results show no significant improvement of SNR for real data because of elevation corrections.

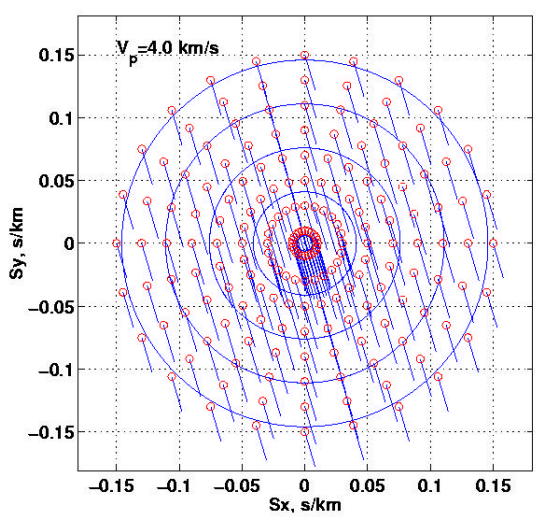

Figure 8. Predicted slowness-azimuth residue vectors induced by ignoring elevation differences at NVAR. Circles represents true values and tails represent observed values.

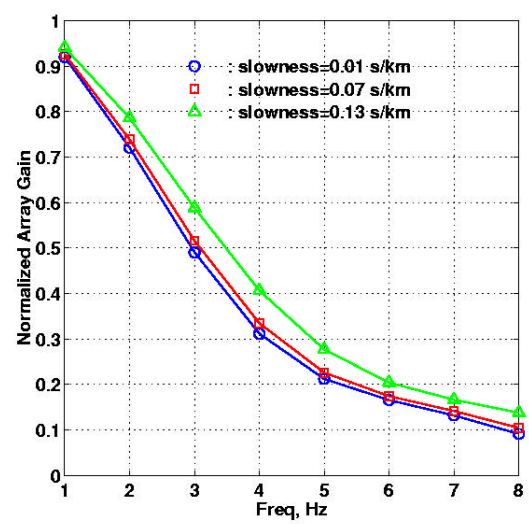

Figure 9. Normalized array gain relative to the ideal array gain at NVAR if elevation differences are ignored. A large reduction in SNR is predicted at frequencies above 2 Hz.

CONCLUSIONS

In this paper we assess the performance of NVAR during its initial few months of operation as part of the IMS using data forwarded to and processed real-time at PIDC. From the standpoint of detection and identification of phases and event location, the array NVAR shows superior performance to its predecessor, the 3-component station MNV. The performance at NVAR is quite comparable to that of similar arrays, like GERES, PDAR and TXAR arrays, which have been operating for some time and have benefited from tuning of their processing.

Preliminary analysis of the new seismic array NVAR suggests that distortion observed in the f-k analysis may be associated with elevation differences across the array. The PIDC processing scheme does, however, allow for removal of slowness biases by applying corrections to observed slowness through SASC's. Development of such corrections for NVAR is currently in progress, which together with evaluation of other aspects of the NVAR real- time processing will likely lead to fine-tuning of several processing configurations.

While predicted elevation effects on beam gain are significant, we have yet to demonstrate that elevation corrections would significantly improve beamforming gain with real data. The observed decay of beam gain with increasing frequency appears to be primarily controled by other factors than elevation.

ACKNOWLEDGEMENTS

We thank Paul Galjan, David Mason and Pierre Caron for their kind assistance.

REFERENCES

Bondár, I., Teleseismic slowness-azimuth station corrections (SASC) for the IMS network, CMR-PRO-98/01, 1998.

Johnson, D. H. and Dudgeon, D. E. (1993). Array signal processing, Prentice-Hall, Inc., Englewood Cliffs, New Jersey.

Wang, J, Israelsson, H. and Carter, J. (1996). A systematic approach to designing detectors for diverse seismic arrays, Seism., Res. Let. 60, No. 2, p60.